

# Investigations of Pulsed Second Sound in Liquid Helium II<sup>\*,\*\*,\dagger</sup>

J. R. PELLAM<sup>\*\*\*</sup>

*Research Laboratory of Electronics, Massachusetts Institute of Technology, Cambridge, Massachusetts*

(Received December 13, 1948)

Pulse methods are applied to the case of second sound in liquid helium II. Both transmitter and receiver consist of thermal elements and d.c. pulses are used throughout. The advantages of pulsing are enumerated for the particular case of second sound. The analogous electrical circuit is formulated for the geometry involved. Data is recorded photographically and examples for several cases presented. Velocity of second sound is given as a function of temperature; both the high temperature and low temperature ranges are extended past those of previous investigators employing standing wave

methods. Attenuation of these d.c. pulses is given as a function of temperature. The "filtering in time" inherent to the pulse method permits the investigation of several forms of coupling between second sound and ordinary sound. The previously known conversion between second sound and classical sound in helium vapor is examined quantitatively. In addition, conversion of second sound to first sound within the liquid is induced by exceeding critical intensities and observed by means of a classical detector. A third conversion, probably occurring upon reflection from a boundary, is illustrated.

## I. INTRODUCTION

IT is well known that liquid helium II is capable of supporting two independent modes of wave propagation. One of these is called first sound and is merely ordinary sound generated and detected by usual acoustical means. The other mode of propagation is called second sound and is unique in being associated primarily with the thermal properties of the liquid. The velocity of second sound is an order of magnitude lower than that of first sound and depends strongly upon temperature.

The theoretical aspects of these properties of liquid helium II have been fully treated in the literature.<sup>1-2</sup> It is sufficient to point out that current theories regard liquid helium II as a mixture of two fluids, called superfluid and normal fluid, and that the two modes of propagation correspond to modes of oscillation of these fluids. For first sound the two fluids vibrate in unison, with the composite liquid "stiffness," or tendency toward equilibrium density,

providing the restoring force in the classical manner. For second sound the two fluids perform a type of internal convection (out of phase with each other) with an "internal stiffness," or tendency toward their equilibrium concentrations, as the restoring force.

The experimental demonstration of the existence of second sound as such was first accomplished by Peshkov,<sup>3</sup> who used thermal methods of excitation and detection, and employed a standing wave technique. Peshkov measured wave velocity as a function of temperature and eventually extended these measurements down to 1.15°K. Second sound was verified experimentally by Lane,<sup>4</sup> who likewise employed resonance methods but used a unique system of detection. Ordinary sound, converted from thermally generated second sound, was detected by an ordinary microphone.

In an effort to extend the velocity measurements in both the high temperature and low temperature directions, and in order to investigate various properties of second sound not readily vulnerable to standing wave methods (such as attenuation and coupling with ordinary types of sound) an alternative experimental approach was developed for the present research. Previous work<sup>5</sup> on the investigation of first sound in liquid helium II had shown a pulse method to have particular advantages. It accordingly appeared that by substituting thermal elements for the piezo-electric transducers employed previously, the inherent advantages of the pulse method could likewise be achieved for second sound. The experiments<sup>6, 6a</sup> conducted proved the method to be even more productive for such "thermal wave" investigations.

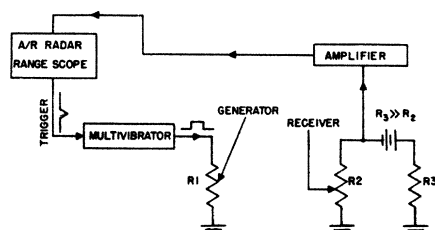


FIG. 1. Block diagram.

\* This research has been supported in part by the Signal Corps, The Air Materiel Command, and ONR.

\*\* This investigation was the outgrowth of a related program originally started with Dr. W. Horvath of the Navy Operations Evaluation Group, while a guest at RLE.

† This work has been described in considerable detail (photographs, curves of velocity and attenuation, etc.) in an RLE Progress Report (reference 6) and has been summarized in a letter to the Editor of this journal (reference 6a).

\*\*\* Now at Cryogenics Laboratory, The National Bureau of Standards, Washington, D. C.

<sup>1</sup> L. Tisza, *J. de Phys. et rad.* **1**, 165, 350 (1940).

<sup>2a</sup> L. Tisza, *Phys. Rev.* **72**, 838 (1947).

<sup>2</sup> L. Landau, *J. Phys. U.S.S.R.* **5**, 71 (1941); also **8**, 1 (1944).

<sup>3</sup> V. Peshkov, *J. Phys.* **10**, 389 (1946); also **8**, 381 (1944); also **10**, 389 (1946).

<sup>4</sup> C. T. Lane, H. Fairbank, H. Schultz, and W. Fairbank, *Phys. Rev.* **70**, 431 (1946) and **71**, 600 (1947).

<sup>5</sup> J. Pellam and C. Squire, *Phys. Rev.* **72**, 1245 (1947).

<sup>6</sup> J. Pellam, M.I.T. Research Laboratory of Electronics Quarterly Progress Report, July 15 (1948).

<sup>6a</sup> J. Pellam, *Phys. Rev.* **74**, 841 (1948).



FIG. 2. Second sound pulse in liquid helium II (data of June 1, 1948). Sweep proceeds from extreme left where generating voltage pulse appears via pick-up. Received signal occurs at right. Intermediate region represents ambient temperature (slope is due to amplifier recovery from initial pulse). Markers represent 61.1  $\mu$ -second intervals. Additional faint signals indicate conversion between first and second sound.

## II. THE PULSE METHOD

The particular capabilities of the method may best be set forth following a brief description of the general technique, illustrating the type of data obtained. Application of pulse techniques to second sound was accomplished by generating heat pulses electrically within liquid helium II and detecting the resultant "thermal waves" as they arrived later at a temperature sensitive receiving element. Standard pulsing methods were employed, including oscilloscopic presentation of the signal, so that large amounts of data could be recorded rapidly by photographic means.

The system is represented in Fig. 1 by a block diagram. Triggers from the DuMont A/R Range Scope simultaneously started the scope time sweep and activated a multivibrator. Video voltage pulses from the multivibrator (of about 150  $\mu$ -seconds duration) were imposed across the resistor  $R_1$ , thereby developing thermal pulses within the adjacent liquid helium II, that is, second sound.

The temperature fluctuations associated with second sound pulses were detected upon arrival at the temperature sensitive carbon<sup>7</sup> resistor  $R_2$ . The

current through  $R_2$  was held essentially constant (about 4 milliamperes d.c.) by means of a much larger series resistor  $R_3$ , so that corresponding voltage pulses were developed. These were sent to an audio amplifier the output of which fed to the vertical plates of the scope.

A typical sample of a second sound pulse is shown in the photograph of Fig. 2, for a fixed distance of 7.57 centimeters between transmitter and receiver and a temperature of 1.653°K. The time sweep proceeds from the extreme left, where the d.c. generating pulse may be seen (as the result of pick-up within the gear). By sufficiently reducing the beam intensity the radar range markers alone appear, so that the trace itself is composed of markers. The first marker represents 48.2  $\mu$ -seconds time delay, and each interval thereafter 61.1  $\mu$ -seconds.

Since the sweep commenced simultaneously with the beginning of the video pulse, the location of the received signal to the right was a measure of the transit time. Thus counting the number of markers between the start of the generating pulse and the beginning of the received signal led to wave velocity.

## III. CAPABILITIES OF METHOD

Departure from standing wave techniques provided features unique to pulsing.

### 1. Direct Reading

Data was taken directly by photographing the screen, in contrast to investigating a standing wave pattern.<sup>3,4</sup> Resultant rapid readings simplified the temperature control problem. The pulse position on the screen was in fact utilized for holding temperature constant in regions near the  $\lambda$ -point where velocity changes rapidly and measurements near to the  $\lambda$ -point obtained.

### 2. Low Heat Input

The low heat input characteristic of pulsing, plus rapidity of measurements, reduced the low temperature restrictions to second sound measurements. Readings in the neighborhood of 1°K were thus accomplished by pumping methods. Ultimate measurements of velocity at the extremely low temperatures attainable by adiabatic demagnetization appear practicable.

### 3. Additional Mechanisms Observable

The isolation of second sound in discrete packets of energy (pulses) and the inherent time delay feature made possible the investigation of various propagation mechanisms otherwise obscured by the system resonances inherent to standing wave methods.

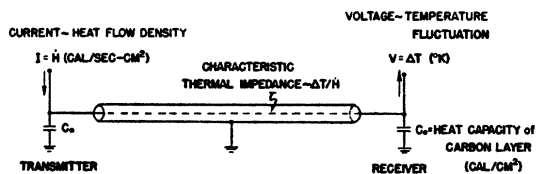


FIG. 3. Analogous circuit (all quantities referred to unit cross-sectional area). [Characteristic Thermal Impedance]<sup>-1</sup> = Characteristic Conductance =  $\zeta c_2$  where  $c_2$  = Velocity of second sound,  $\zeta$  = Specific heat per cc for helium II. The wave equation  $\nabla^2 T = 1/c_2^2 (\partial^2 T / \partial t^2)$  associated with this transmission line reduces to Poisson's equation  $\nabla^2 T = 0$  for the zero frequency case, with solution  $T = \text{constant}$ . This corresponds to the constant electrical potential within a perfect conductor (or uniform pressure within a compressed gas for the acoustical case) and illustrates the inadequacy of early heat conduction experiments based on steady state heat flow. ( $C_2$  should be expressed in units of cal./cm<sup>3</sup> deg.)

<sup>7</sup> H. A. Fairbank and C. T. Lane, Rev. Sci. Inst. 18, 525 (1947).

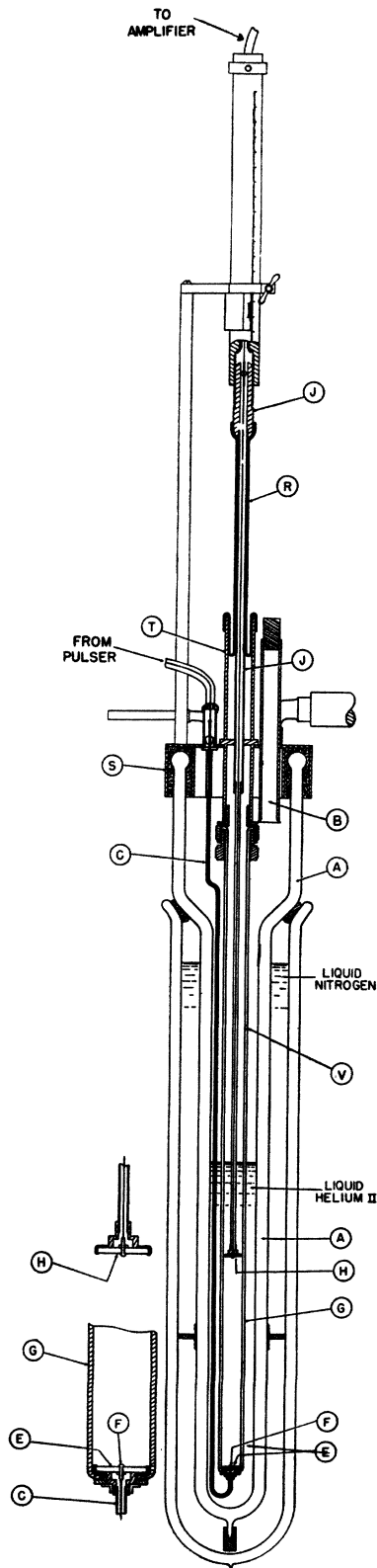


FIG. 4. Apparatus with movable receiving element for measurements between 1.5°K and the  $\lambda$ -point.

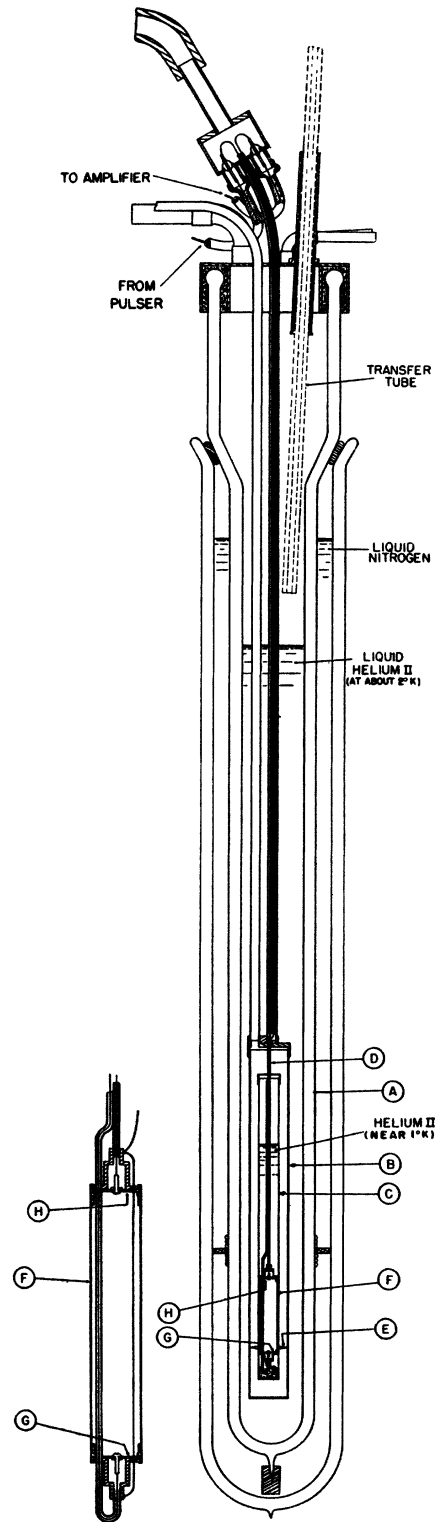


FIG. 5. Apparatus for measurements below 1.5°K.

Thus by observing the diminution in amplitude of independently progressing pulses, attenuation

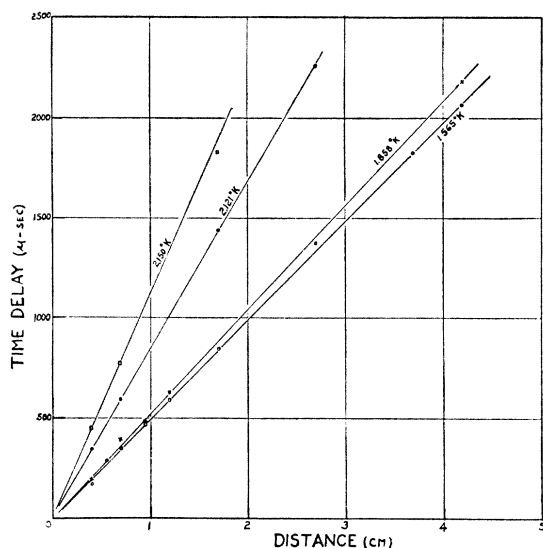


FIG. 6. Elapsed time delay *versus* transit distance for various temperatures (data of June 8, 1948). Zero intercept illustrates absence of significant inherent time delays.

has been measured and its temperature dependence determined. Likewise coupling phenomena between second sound and ordinary sound were isolated sufficiently for quantitative study. Three different types of such coupling have thus far been observed. The transit time of any particular signal identified it definitely with the type of wave motion involved, by virtue of the known difference in wave velocities.

#### IV. OPERATING CONSIDERATIONS

##### Heat Input (Optimum Conditions)

Low heat input may be attributed to the following. First, all thermal energy of d.c. pulses appears as second sound; for sinusoidal generating currents, on the other hand, equal amounts of energy go to second sound (at twice the impressed frequency) and to continuous heating. Next, the intermittent nature of pulsing results in low average power for high peak power. Finally, rapid recording of data reduces the total heating interval.

Heat is introduced by the receiver as well as by the transmitter, due to its constant d.c. current (maintained during photographic exposure). Optimum conditions (minimum total heating for given received signal strength) occur when the average transmitter heating is twice the average receiver heating. For pulsed systems this allows reduction in total average heating without sacrificing peak power signals.

##### Analogous Circuit

It was necessary for design to evaluate quantitatively the function of the liquid helium portion of the total circuit (Fig. 1). The nature of the thermal

wave allows a complete analogy to electrical propagation, resulting in a characteristic *thermal impedance* for second sound; that is, temperature fluctuation replaces voltage, and heat flow per unit area replaces current so that the *thermal impedance* is the ratio of the two. The reciprocal quantity, intensity of heat flow per temperature change, is *thermal conductance*. It was learned near the completion of this program that a quantity identical to *thermal impedance* had been derived independently and checked by Osborne,<sup>8</sup> so that the present discussion concerns only the analogous circuit.

The circuit applies to unit cross section area of fluid and becomes, for the particular geometry, a transmission line terminated in capacitances  $C_0$  at either end.<sup>††</sup> Numerically  $C_0$  is the unit area heat capacity of a thin carbon surface layer. Thermal impedance depends upon known properties of liquid helium II (see Fig. 3), so that temperature fluctuations (and therefore signal strength) were predicted, based on the "analogous current"  $\dot{H}$  of heat flow per unit transmitter area.

#### IV. EQUIPMENT

##### Apparatus Employed between 1.5°K and the $\lambda$ -Point

Separate equipment was employed for the measurements above and below 1.5°K. For above 1.5°K the receiver element was movable relative to the transmitter, a sectional view of the apparatus appearing in Fig. 4. The apparatus is shown supported on the inner glass Dewar *A* which contained the liquid helium. Liquid helium was admitted by inserting the transfer tube of the Collins Cryostat through the opening provided by tube *B*, later sealed as shown for applying vacuum.

Video pulses from the multivibrator were fed down the small coaxial line *C* to the disk *E* acting as the generator of second sound. This disk was composed of resistance strip (carbon layer<sup>7</sup> on Bakelite base) of 800 ohms per square. The voltage pulses were fed to the center terminal *F* of this disk and developed a radial current flow to the circumference which was grounded. Carbon-to-metal contacts were assured at both the center and edge of the disk by means of silver paste electrodes, and mechanical support by a narrow brass rim spun over the periphery.

The second sound pulses were constrained to travel within the glass tube *G* which also provided a guide for the receiving element *H*. This receiver was identical to the transmitting element, consist-

<sup>8</sup> D. Osborne, *Nature* 162, 213 (1948).

<sup>††</sup> Assuming that the thermal resistivity of the carbon layer was greatly exceeded by that of its Bakelite backing; otherwise dissipative circuit elements would enter.

ing also of a carbon coated disk. Here however advantage was taken of the temperature dependence of the carbon surface resistance. The center conductor (leading from the midpoint of the receiver disk *H*) carried the resultant pulses through a vacuum seal to the amplifier.

Actually because of complete top-to-bottom symmetry, the roles of transmitter and receiver were occasionally interchanged. In order to keep the propagation essentially one-dimensional, the exposed carbon surfaces of the disks extended to within less than one millimeter from the glass guide, of inner diameter five-eighths inch.

The entire receiver mounting could be moved vertically and clamped at any desired position. A vacuum seal was provided for all positions of the receiver by means of the crude rubber tubing *R* fitted about tube *J* and attached to cap *S* via the short tube *T*; vacuum seal to the Dewar *A* itself resulted from a rubber sleeve (not shown) fitting over *S* and squeezed tight about the glass.

Zero setting, corresponding to coincidence of the two disks, was checked during each run by lowering the receiver until the center electrodes made electrical contact; an additive constant was obtained from x-rays of the gear in the same position.

Temperature was determined by reading vapor pressure. For this it was essential that liquid helium *II* inside the glass guide *G* remain in complete equilibrium with the liquid helium outside, where pumping and manometric readings occurred. Accordingly tube *G* was perforated by two small holes, one considerably above the liquid surface, and the other beneath the level of transmitter *E*. The upper hole *V* assured vapor pressure equilibrium, and the lower *V'* maintained temperature equilibrium within the liquid. Like liquid levels inside and outside evidenced this desired condition.

#### Apparatus Employed below 1.5°K

The majority of the results were obtained with the previously described equipment. However for attempting the determination of velocity behavior at extremely low temperatures, equipment was later constructed along known lines for attaining lowest temperatures by pumping. As shown in Fig. 5 the essential portions of the apparatus were unchanged, except that constant transmitter-receiver separation was employed.

Especially long glass dewars were constructed for this phase of the program. Suspended within the inner one *A* was a metal container *B*, surrounding in turn an inner metal capsule *C* for lowering helium temperatures to 1°K. Liquid helium was condensed into this container *C* under slight pressure through the narrow neck *D*, using roughly one millimeter of helium transfer gas for thermally

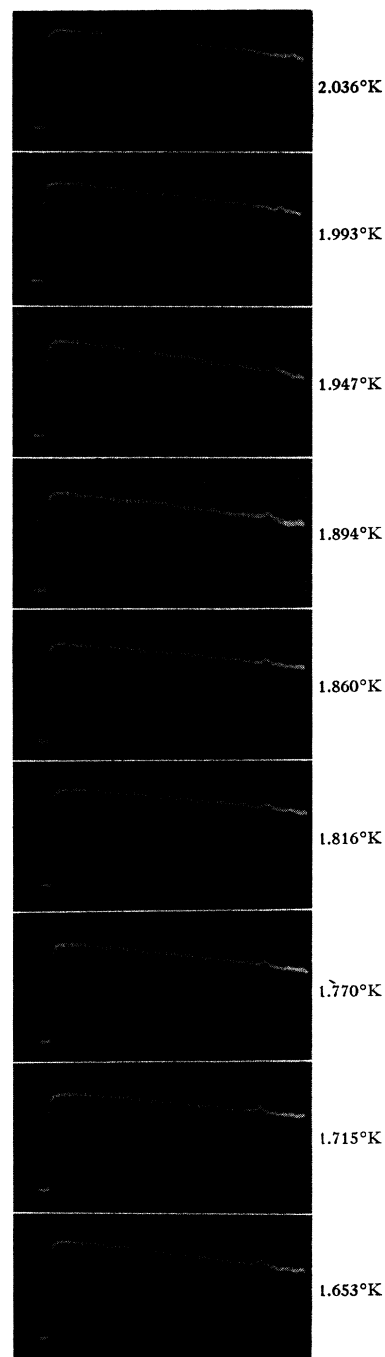


FIG. 7. Second sound pulses at various temperatures for fixed transmitter-receiver distance of 7.57 centimeters (data of June 2, 1948). The trend with temperature is evident.

connecting *B* and *C*. Thermal isolation was then provided by evacuating this intermediate space with a diffusion pump so that heat could flow to the measurement chamber only via the narrow tube *D* (one millimeter diameter) or through the needle supports *E*. Naturally heat was introduced elec-

trically during pulsing and detection of second sound.

Within chamber *C* was a second sound cell *F* of fixed path-length 5.190 centimeters. Electrical leads to the transmitter *G* and the receiver *H* passed unshielded through the narrow neck *D*; intercoupling was, however, unimportant since resulting pick-up occurred before the pulse reached the receiver for detection. Shielded conductors led through vacuum seals to outside co-axial lines.

Temperature equilibrium was assured inside the measurement chamber by means of small perforations through the transmitter and receiver disks. However, due to the haste in construction it was not possible to provide accurate temperature measuring elements within the inner chamber, and the values deduced from vapor pressure readings are subject to considerable uncertainty.

## V. EXPERIMENTAL RESULTS

### A. Velocity Measurements

#### 1. Extraneous Time Lag Absent

Before interpreting the ratio of transit distance to transit time directly as second sound wave velocity, it was necessary to establish the absence

of extraneous time delays. This is demonstrated in Fig. 6 where total delay time is plotted *versus* path length for various temperatures. Extrapolation gives a series of straight lines converging near the origin and indicates that any additional time delays occurring during formation or detection of the pulses were negligible compared to the transit times (three to four thousand  $\mu$ -seconds for velocity measurements). Alternatively, velocities based on increments in time delay for known increments in path length agreed with those of the more direct method.

Furthermore the elapsed time to the beginning of the primary signal was independent of pulse duration (at least for 30  $\mu$ -seconds or more), pulse repetition frequency, and input transmitter voltage. This was in line with Peshkov's results, which indicated absence of frequency dispersion.

#### 2. Velocity as a Function of Temperature

The temperature dependence of second sound velocity near the  $\lambda$ -point is demonstrated in Fig. 7, showing signals for related temperatures. Spaced approximately 0.05°K apart, these photographs show an orderly decrease of wave velocity with increasing temperature (since the delay time increased, distance remaining fixed).

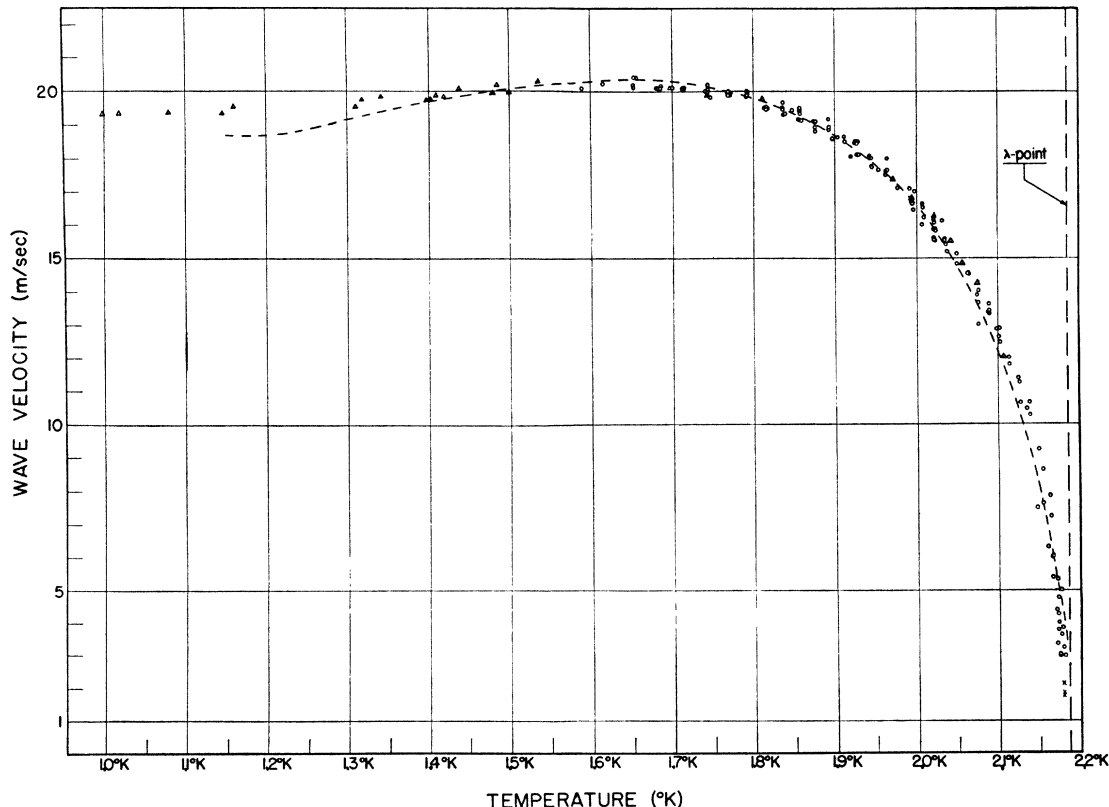


FIG. 8. Second sound wave velocity *versus* temperature. Dotted line indicates Peshkov's results; circles represent present measurements obtained with equipment of Fig. 4; triangles represent present measurements obtained with equipment of Fig. 5.

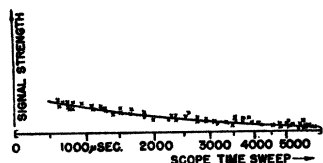


FIG. 9. Attenuation: Signal strength *versus* time delay for constant temperature ( $T=2.134^{\circ}\text{K}$ ) (data of June 17, 1948). Crosses represent data from individual motion picture frames. Note decrease in signal strength with increased transit distance.

The composite results of a large number of measurements of velocity are plotted in Fig. 8, where each point represents an individual photographic determination. Different symbols are used to represent values obtained with the two sets of equipment, in order to differentiate in terms of reliability. Thus circles indicate values measured with the apparatus of Fig. 4, for which temperature determinations are reliable; direct vapor pressures measured at the free HeII surface preclude systematic errors. On the other hand values represented by triangles were obtained with the equipment of Fig. 5, for which "manometric temperatures" indicated may have deviated from the true temperatures, due to the narrow pumping tube  $D$ .

Although the circles are restricted to the higher temperature range between  $1.5^{\circ}\text{K}$  and the  $\lambda$ -point, the triangles cover the entire temperature range. The marked correlation between the circles and the dozen odd triangles appearing above  $1.5^{\circ}\text{K}$  clearly indicates the reliability of temperatures measured in this upper range through the narrow neck  $D$ . Any temperature aberrations arising in this equipment (Fig. 5) may thus be associated with the extreme low temperature range only.

For purposes of comparison, Peshkov's results are given by the dotted line. Nearly complete agreement between the two sets of data is evident in the range from  $1.4^{\circ}\text{K}$  to the  $\lambda$ -point, where present results deviate only slightly from Peshkov's. The small variations appear to be systematic, and the present determinations are presented in numerical form in Table I. Each velocity value is the average of several (three to twelve) separate measurements.

Velocity measurements as low as three meters per second were attained from still photographs. By recording the signal behavior with motion pictures while passing in and out of the  $\lambda$ -point (transit distance of millimeters), velocities below two meters per second were observed. The latter are marked as crosses on the extension of the curve toward zero.

In contrast to the results above  $1.4^{\circ}\text{K}$ , the velocity measurements at the lower temperatures deviate markedly from those of Peshkov. This points strongly to temperature discrepancies in the present lowest temperature determinations and

makes these values significant only with reservations. Thus no numerical values are given in Table I for temperatures below  $1.4^{\circ}\text{K}$ . Could the similar flattening of Peshkov's velocity curve originate in like causes?

## B. Attenuation Measurements

### 1. Decay of Second Sound Pulses

By lifting the receiver of Fig. 4 vertically through the liquid helium II as pulses were being sent from

TABLE I. Measurements of the velocity of second sound at various temperatures.

Temperature ( $^{\circ}\text{K}$ )	Velocity (m/sec.)	Temperature ( $^{\circ}\text{K}$ )	Velocity (m/sec.)
2.176	$3.12 \pm 0.07$	1.955	$17.78 \pm 0.06$
2.174	$3.91 \pm 0.08$	1.925	$18.35 \pm 0.08$
2.170	$5.00 \pm 0.14$	1.900	$18.78 \pm 0.07$
2.163	$6.91 \pm 0.40$	1.877	$18.89 \pm 0.05$
2.158	$7.57 \pm 0.09$	1.858	$19.29 \pm 0.06$
2.153	$9.01 \pm 0.17$	1.837	$19.46 \pm 0.06$
2.146	$10.54 \pm 0.07$	1.806	$19.68 \pm 0.07$
2.121	$11.63 \pm 0.14$	1.771	$19.91 \pm 0.03$
2.105	$12.64 \pm 0.30$	1.745	$19.99 \pm 0.05$
2.084	$13.65 \pm 0.08$	1.698	$20.10 \pm 0.01$
2.056	$14.83 \pm 0.10$	1.654	$20.26 \pm 0.08$
2.027	$15.78 \pm 0.06$	1.603	$20.07 \pm 0.04$
2.000	$16.77 \pm 0.09$	1.489	$20.06 \pm 0.03$
		1.408	$19.83 \pm 0.03$

the transmitter, a decrease in signal strength could be observed with increased path-length. The one-dimensional characteristics of the propagation precluded geometrical attenuation due to wave divergence. Accordingly such losses in signal strength were ascribed to true liquid attenuation.

Motion picture records of the screen were taken as the receiver was thus raised. For analysis each individual frame was projected against a screen, and the height of the signal marked. Successions of such markings resulted in curves as illustrated in Fig. 9. Experience showed that the temperature of the liquid bath remained virtually constant during this procedure, satisfying isothermal requirements. For this sample the ambient temperature was  $2.134^{\circ}\text{K}$ . The scale factor relating time-delay (indicated on the scope) to actual distance between transmitter and receiver was of course the known second sound velocity.



FIG. 10. Second sound pulses showing primary signal plus first echo (data of June 11, 1948). Temperature of  $2.164^{\circ}\text{K}$  and path-length of 0.374 centimeter. (Generating pulse markedly reduced by greater electrical shielding.)

Signal strength thus plotted was a direct indication of temperature fluctuations accompanying second sound pulses. Accordingly a measure of the exponential "temperature attenuation coefficient"  $\alpha$ , defined by the equation

$$\Delta T = \Delta T_0 e^{-\alpha x} \quad (1)$$

was obtained for second sound pulses, where  $\Delta T$  is not to be confused with the ambient temperature  $T$ , and  $x$  is distance in centimeters.

Alternative attenuation determinations were obtained from photographs showing multiple echoes. Thus Fig. 10, for a temperature of 2.164°K and transit distance of 0.374 centimeter, demonstrates multiple reflections and multiple excursions for second sound. The echo shows the attenuating effect of the triple path-length resulting in annihilation of subsequent echoes.

## 2. Attenuation as a Function of Temperature

From data like Fig. 9 the exponential "temperature attenuation coefficient"  $\alpha$  was evaluated for the temperature range from 1.65°K to the  $\lambda$ -point. Fig. 11 gives  $\alpha$ , plotted in units of reciprocal centimeters, *versus* the ambient liquid temperature  $T$ . The results were for pulses of approximately 150  $\mu$ -seconds duration and repetition rate 78 per second.

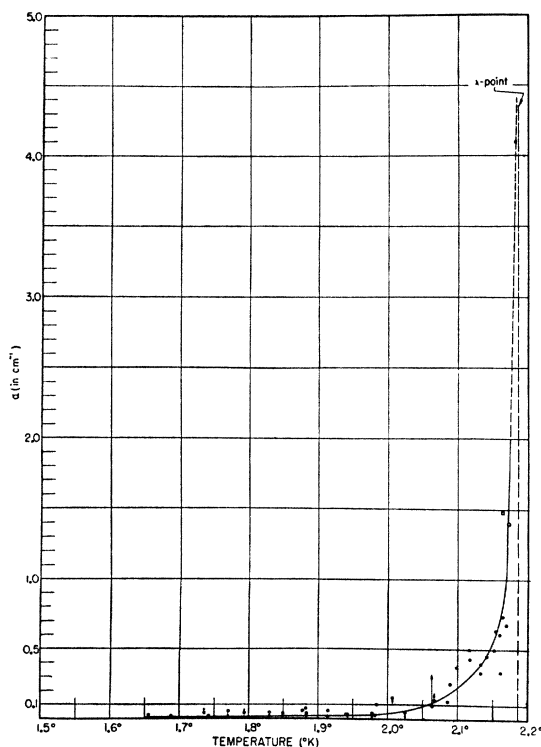


FIG. 11. Attenuation coefficient  $\alpha$  ( $\text{cm}^{-1}$ ) *versus* temperature (data of June 17, 1948) for 150  $\mu$ -sec. pulses at 78/sec. p.r.f. Circles for variable path-length data; squares for multiple reflection data; curve represents reasonable mean value.

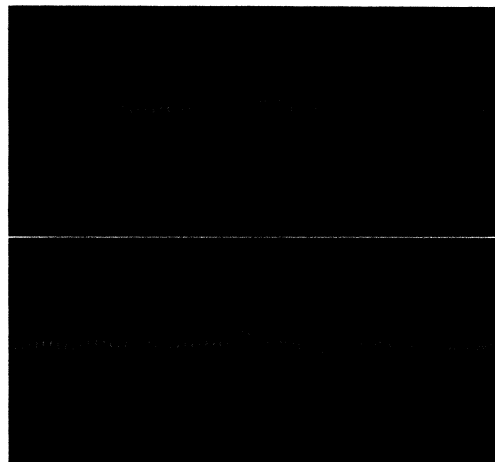


FIG. 12. Surface conversion: Comparison between pulses detected within liquid and within vapor ( $T=2.023^\circ\text{K}$ ) (data of June 18, 1948). Upper photograph for receiver above surface. Lower photograph for receiver beneath surface.

Additional data from multiple echoes (as in Fig. 10) are plotted in squares. For these alternative determinations complete reflectivity was assumed for each end of the second sound path.

Attenuation is extremely small over most of the temperature range investigated, being an amplitude decrease per centimeter of less than one percent at 1.65°K (0.2 decibel per centimeter). Apparent however is a consistent increase with increased temperature, setting in especially above 2.0°K and leading to probably infinite value at the  $\lambda$ -point. The highest measured value of  $\alpha$  was 4.1  $\text{cm}^{-1}$ . This strong attenuation suffered by the pulses in approaching the  $\lambda$ -point provides a natural annihilation of second sound, forbidden in the helium I phase setting in above 2.19°K.

## C-1. Conversion at Surface

### 1. Detection in Vapor

The conversion phenomenon previously observed by Lane to occur at the interface between liquid helium II and its equilibrium vapor was studied by pulse methods. Both media appeared infinite to pulses, so that system resonances were avoided and surface conversion proceeded quite independently of the geometry.

As the movable receiver of Fig. 4 was lifted vertically through the liquid surface and out into the vapor, the signals from second sound pulses below gave way to signals from classical sound within the vapor. Although the thermal detector was insensitive to ordinary sound (first sound) in the liquid, where the specific heat ratio barely exceeds unity, this was not the case for classical sound generated in the vapor above, where the ratio is five-thirds.



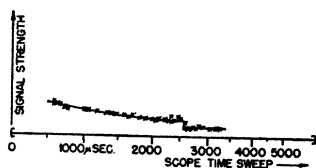


FIG. 13. Surface conversion: Temperature fluctuation *versus* time delay ( $T=2.162^{\circ}\text{K}$ ). Sharp drop in signal strength represents emergence of receiver from liquid to vapor above.

Figure 12 shows a set of signals, one the second sound pulses detected within the liquid, and the other the pulses detected by the same thermal element when lifted into the vapor.

Methods identical to those employed for measuring second sound decay resulted in curves such as shown in Fig. 13, where temperature fluctuations are plotted (in arbitrary units) *versus* time delay. The effects of pulling the receiving element through the surface are apparent.

By recording a series of still photographs with the receiving element in the vicinity of the surface, the time delay accompanying this process may be plotted *versus* the position, as in Fig. 14.

## 2. Observed Boundary Conditions

The behavior of the received signal in the vicinity of the surface provides insight to the boundary conditions holding during the conversion process. Plots of signal strength *versus* position (Fig. 13) indicate amplitudes of temperature fluctuation from the ambient to be of like order of magnitude in the liquid and in the vapor. The dozen observations made in the range from  $1.7^{\circ}\text{K}$  to the  $\lambda$ -point show "temperature amplitudes" in the vapor pulses to have been actually one-half those in the second sound pulses arriving from the transmitter. Virtually no dependence upon ambient temperature was evident.

Similarly transit times plotted *versus* position revealed the instantaneous nature of the process (delays were measured to the center of signal pulses so that results were independent of possible pulse shape alterations), as illustrated by Fig. 14 for  $2.023^{\circ}\text{K}$ . The intersection of the two relationships without discontinuity at the surface indicates no associated time lag.

## C-2. Conversion at Transmitter

### 1. Overdriven Second Sound

A conversion from second sound to first sound within the liquid helium II is demonstrated in Fig. 15, obtained by substituting a classical (vibration) microphone for the thermal receiving element. This well illustrates the "time filtering" aspect of pulse methods; the path length and scope time sweep were identical to those of Figs. 2 and 7,

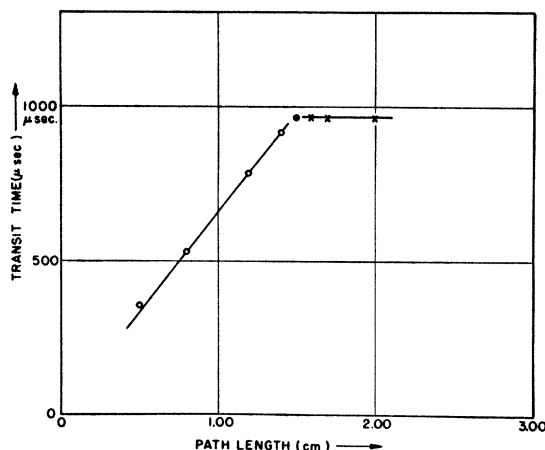


FIG. 14. Surface conversion: Transit time *versus* path length ( $T=2.023^{\circ}\text{K}$ ). Circles for receiver in liquid; crosses for receiver in vapor; dot for position of receiver not certain, probably in liquid.

but the primary pulse position associates the propagation unmistakably with the high wave velocity of first sound.

Although the presence of second sound itself was not revealed directly by the vibration microphone (undetectable second sound was present when Fig. 15 was taken, in the same manner that undetectable first sound was present when Figs. 2 and 7 were taken) the phenomenon was associated closely with the thermal properties of liquid helium II. Thus for example it disappeared abruptly above the  $\lambda$ -point (a faint signal was actually obtained above the  $\lambda$ -point, but orders of magnitude weaker).

### 2. Breakdown Conditions

The hypothesis of the first sound generation by internal degeneration of second sound was furthered by the non-linear characteristics of the process. Figure 16 shows the observed signal strength (first sound amplitude) as a function of input voltage to the transmitter. Below the lower critical limit of three volts no effect is observable; above this value the signal increases with voltage in an orderly fashion. Insufficient data has been taken for establishing any temperature dependence

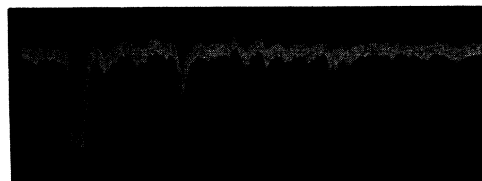


FIG. 15. Presence of first sound detected by vibration microphone ( $T=2.09^{\circ}\text{K}$ ). Note short time delay due to higher velocity.

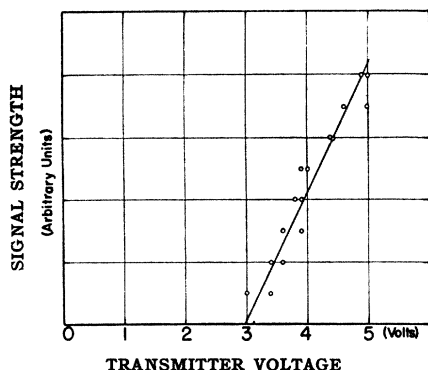


FIG. 16. First sound signal amplitude *versus* transmitter voltage (data of May, 1948) ( $T = 2.09^\circ\text{K}$ ).

of the critical voltage; results thus far would suggest little variation.

Regarding the actual time processes involved, the position on the screen was found to be quite independent of pulse width, pulse repetition frequency, and power input (as was the second sound signal previously discussed). There was however evidence of time delay. On the basis of the first sound only, computed velocities were somewhat lower than known values, especially at temperatures just below the  $\lambda$ -point. Attributing this obvious delay to a portion of the path traversed as second sound, it was found that the conversion evidently takes place about one-fourth millimeter from the transmitter surface. This distance does not change appreciably in the range from  $1.7^\circ\text{K}$  to the  $\lambda$ -point, resulting in the larger time delays from lower second sound velocities near the  $\lambda$ -point.

### C-3. Conversion upon Reflection

#### 1. First Sound Converted to Second Sound

The faint signals roughly nine range markers behind the primary signals of Fig. 7 indicate still another conversion. The separation between signals corresponds to first sound transit time, including the above-mentioned delay during formation. Signals were evidently generated at the receiver by pick-up between the leads to the transmitting and receiving elements (see start of sweep in Fig. 7 where receiver amplifier was driven to saturation). Upon arrival at the actual transmitter surface, these first sound pulses were reflected with partial conversion to second sound. Arriving back at the receiver, the resultant second sound pulses were detected thermally and recorded with delay times corresponding to one first sound transit plus one second sound transit. That the entire process in this speculation could not have been in reverse seems likely in view of the d.c. detecting current existing only at the receiver.

## VI. INTERPRETATIONS AND CONCLUSIONS

In fairness to the pulse method it is mentioned that the full potentialities of the technique were not attained during this research, which was conducted under difficult experimental conditions.

In fact it is entirely likely that second sound was first observed using an impulse method, by Ganz<sup>9</sup> while measuring heat conductivities. Ganz discharged a condenser through a resistor in liquid helium II and detected a thermal impulse one meter distant within 0.05 sec., but apparently overlooked the wave nature of the phenomenon.

### A. Velocity

In the upper temperature range the agreement with Peshkov's results is satisfactory. The present velocities appear to approach zero somewhat more abruptly at the  $\lambda$ -point, as indicated by the lowest values. Also a slightly lower maximum value was obtained. That the present results show deviations both above and below those of Peshkov is evidence against any source of systematic error, as would arise from extraneous time delays, in the range from  $1.4^\circ\text{K}$  to the  $\lambda$ -point.

The primary purpose of extending the velocity measurements to extreme low temperatures was to detect any gross increase or decrease in velocity. Both of the present theories<sup>1,2,10</sup> predict strong variations, but in opposite directions. In this respect it was felt that approximate low temperature determinations would suffice to reveal such trends. The apparent small velocity dependence "near  $1^\circ\text{K}$ ," however, defeats this objective, probably because of temperature uncertainties. A decisive answer apparently awaits the application of pulse methods to paramagnetically cooled liquid helium.

### B. Attenuation

#### 1. Theoretical Considerations

It is not possible at this juncture to correlate the observed attenuation with theoretical predictions. Even if an adequate theory did exist, the broad frequency characteristics of the d.c. pulse spectrum would obscure the frequency dependence. However, certain speculations can be made.

In a paper<sup>5</sup> with Squire on attenuation of first sound in liquid helium II, it was explained that absorption might be expected there because of viscosity, but that the virtually isothermal nature of first sound precluded absorption by heat conduction. Values computed on this entirely classical basis failed to account for the observed first sound attenuation, thereby suggesting other second order effects, probably disequilibrium between the two liquid components.

<sup>9</sup> E. Ganz, Proc. Camb. Phil. Soc. **36**, 127 (1940).

<sup>10</sup> E. Lifshitz, J. Phys. U.S.S.R. **8**, 110 (1944).

For second sound the situation is more complicated, since inherent temperature fluctuations should enhance absorption by second order heat conduction (irreversible heat flow by diffusion within the normal fluid component). Furthermore the variations from equilibrium concentration of the fluid components should produce absorptive transitions between the two. Both of these have been suggested by Tisza.<sup>1a</sup>

For concreteness the expected attenuation due to viscosity is derived for a single frequency  $\nu$ :

$$\alpha_{vis} = (8\pi^2\eta_n\nu^2/3\rho c_2^3)(\rho_s/\rho_n). \quad (2)$$

This expression is identical to that for first sound absorption, except for the replacement of first sound velocity by second sound velocity  $c_2$  and the additional factor  $\rho_s/\rho_n$  accounting for the manner in which momentum and energy are shared between the component fluids;  $\rho_s/\rho_n$  is the ratio of superfluid density to normal fluid density,  $\rho$  the total density, and  $\eta_n$  the viscosity coefficient of the normal fluid component (see reference 5).

All of the absorption mechanisms depend thus inversely upon the third power of wave velocity, so that relatively high absorption of second sound should be expected (the velocity being one or two orders of magnitude less than for first sound). The low values plotted in Fig. 11, result entirely therefore from the low frequencies composing the pulse spectrum (below several kilocycles). Assuming the usual frequency squared dependence, second sound should be absorbed drastically in the megacycle range.

The presence of wave velocity in the denominator of (2) also accounts qualitatively for the observed sharply increased attenuation near the  $\lambda$ -point (where  $c_2$  approaches zero). The  $\rho_s/\rho_n$  factor partially counteracts this rise for the case of viscosity, so that additional absorption mechanisms must play predominant roles.

## 2. Present Object and Limitations

The purpose of the present attenuation investigation was to establish the dependence upon temperature. It is emphasized that these were rough measurements and that for precise work pulsed c.w. rather than pulsed d.c. should be employed. The resulting elimination of a broad frequency spectrum, with its probably selective absorption, should improve accuracy. Such scatter as appears in Fig. 11 is probably attributable to this source (deviation from true exponential decay). Extreme uncertainty is indicated by arrows, so that  $\alpha$  at lowest temperatures lies between the circles at maximum values and zero.

The application of pulsed c.w. would likewise determine the frequency dependence and would

specify the constant factor fixing the absolute magnitude of  $\alpha$ .

## C-1. Conversion at Surface

### 1. Boundary Condition Indicated

On the basis of such data as Figs. 12 and 13, it was stated that the vapor pulses appeared to possess roughly one-half the temperature fluctuation from the ambient of the second sound pulses originally arriving at the surface. The consistency with which this amplitude ratio remains unchanged over a wide temperature range strongly suggests a boundary condition. That this boundary condition might actually be a continuity of temperature at the surface, apparently reduced to one-half by instrumental factors, must not be overlooked.

Interpreting the observed values as direct temperature ratios requires the tacit assumption that the receiving element behaves identically in both liquid and vapor. The quite different thermal properties of the two media might cause the receiver to modify the two modes of propagation differently, presumably lowering the measured ratio. As may be seen from Fig. 12, the slight change in pulse shape appears insufficient to halve the ratio.

## C-2. Conversion at Transmitter

### 1. Breakdown of Second Sound Observed

The virtual disappearance above the  $\lambda$ -point of first sound signals detectable by a vibration microphone (Fig. 15) clearly indicates a mechanism depending upon the particular thermal properties of liquid helium II. Evidently the high *thermal conductance* of liquid helium II provides means for injecting thermal energy from the transmitter surface into the liquid mass. The mass transfer characteristics of this orderly heat flow (second sound), involving only relative densities of the fluid components, appears to degenerate; the resultant less ordered heating provides the over-all density fluctuations of first sound. Such a process is expected on the basis of Kapitza's<sup>11</sup> experiments on breakdown of superfluid flow through narrow apertures; this was in fact predicted by Peshkov<sup>3</sup> for the internal convection of second sound.

### 2. Critical Heat Flow Density Indicated

By analogy to Kapitza's observations, internal turbulence between the fluid components ought to occur only above critical relative particle velocities. That is, liquid helium II supports heat flow up to a certain critical density above which internal friction sets in. This is apparent in Fig. 16 where first sound generation, once commenced, increases regu-

<sup>11</sup> P. Kapitza, J. Phys. U.S.S.R. 5, 59 (1941).

larly with heat flow density. Like results for frictional retardation were observed by Kapitza<sup>11</sup> with regard to a critical superflow velocity.

Only an order of magnitude value for critical heat flow density may be given at this time. At 2°K the internal convection appears to have suffered degeneration at a heat flow density of about 0.0025 cal./cm<sup>2</sup> sec. This is less than used by Lane,<sup>4</sup> thus possibly explaining his detection of first sound by a completely submerged microphone.

Continued measurements in this direction are expected to provide detailed information on the critical relative velocities of the two fluids during the internal convection process.

### C-3. Conversion upon Reflection

Finally the faint signals of Fig. 7 show that by some process first sound has been converted to second sound during reflection from the carbon coated Bakelite surface. No explanation for this is attempted; it is not known whether the carbon surface might be sufficiently penetrable to superfluid for the conversion expected at a porous surface<sup>12</sup> to have occurred.

<sup>12</sup> J. Pellam, Phys. Rev. **73**, 608 (1948).

### VII. ACKNOWLEDGMENTS

Space does not permit adequate acknowledgment to all those contributing in one way or another to this program. Professor Slater's sincere interest at all times provided an encouraging influence, particularly during the more difficult early phases. Guests at the laboratory prior to this program, Drs. M. Desirent and W. Horvath, introduced and refined many low temperature techniques and developed helium transfer methods. At the suggestion of Professor Tisza, Dr. Horvath and the author undertook an early investigation to measure second sound wave velocities at very low temperatures, using established standing wave methods. Dr. Horvath's work in this connection (plus organizing a program for adiabatic demagnetization) cannot be over-rated.

Following his departure, emphasis was shifted to second sound measurement techniques, and the pulse method developed. The author conducted this program with the technical assistance of R. Cavileer and P. Nicholas. The former furnished liquid helium on repeated occasions, while the continued willing support of P. Nicholas in all phases of the final program contributed markedly to the eventual results.

## The Hyperfine Structure of Tritium

EDWARD B. NELSON AND JOHN E. NAFE  
*Columbia University, New York, New York*

(Received January 10, 1949)

The hyperfine structure of the ground state of tritium was measured by the atomic beam magnetic resonance method. The frequency of the field independent central Zeeman component of the transition ( $F=1 \leftrightarrow F=0$ ) gives the h.f.s. almost exactly with a field correction of less than 0.001 Mc. The mean of three independent determinations of the h.f.s. in different weak magnetic fields is  $1516.702 \pm 0.010$  Mc. The probable error is caused by the uncertainty in the Doppler correction and possible asymmetry in the resonance lines causing a shift in the center of the line. The reproducibility of determining the center of the resonance line was  $\pm 0.002$  Mc. The theoretical value of the h.f.s. based on the triton-proton moment ratio and the value of the h.f.s. of hydrogen is  $1516.709 \pm 0.015$  Mc. The theoretical and experimental values agree within the probable error of the moment ratio, 1 part in  $10^5$ , which also proves that the spin of the triton is  $\frac{1}{2}$ .

### INTRODUCTION

THE hyperfine structure of the ground state of tritium has been measured by the atomic beam magnetic resonance method<sup>1</sup> previously employed by the authors<sup>2</sup> in the case of H and D. A measurement of the h.f.s. is well suited to test the theory of the h.f.s. of the hydrogens as it has been extended in the light of the results obtained with H and D.

<sup>1</sup> P. Kusch, S. Millman, and I. I. Rabi, Phys. Rev. **57**, 765 (1940).

<sup>2</sup> J. E. Nafe and E. B. Nelson, Phys. Rev. **73**, 718 (1948).

The h.f.s. separation in absolute frequency units for the  $^2S_{\frac{1}{2}}$  state of a hydrogenic atom having infinite nuclear mass has been calculated by Fermi<sup>3</sup> and is given by

$$\nu = [8\pi/3h][(2I+1)/I]\mu_N\mu_0\psi^2(0), \quad (1)$$

where  $I$  is the nuclear spin in units of  $\hbar$ ,  $\mu_N$  and  $\mu_0$  the nuclear and electronic magnetic moments, respectively, and  $\psi(0)$  the Schrödinger wave function evaluated at  $r=0$ .

The effect of the relative motion of the nucleus

<sup>3</sup> E. Fermi, Zeits. f. Physik **60**, 320 (1930).

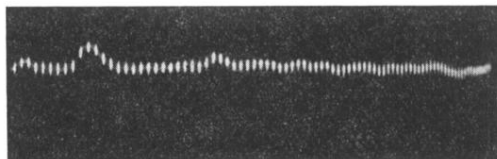


FIG. 10. Second sound pulses showing primary signal plus first echo (data of June 11, 1948). Temperature of  $2.164^{\circ}\text{K}$  and path-length of 0.374 centimeter. (Generating pulse markedly reduced by greater electrical shielding.)

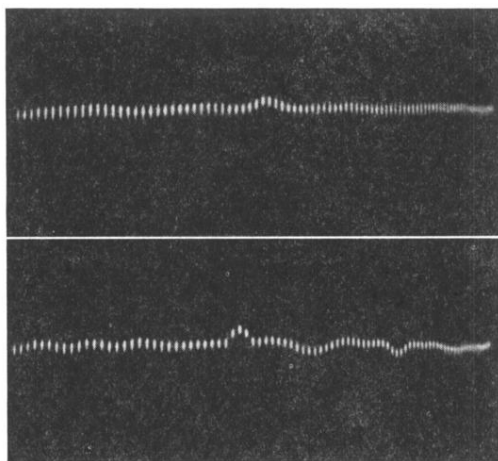


FIG. 12. Surface conversion: Comparison between pulses detected within liquid and within vapor ( $T=2.023^{\circ}\text{K}$ ) (data of June 18, 1948). Upper photograph for receiver above surface. Lower photograph for receiver beneath surface.

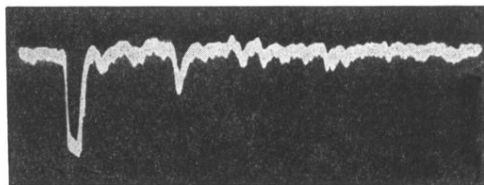


FIG. 15. Presence of first sound detected by vibration microphone ( $T=2.09^{\circ}\text{K}$ ). Note short time delay due to higher velocity.

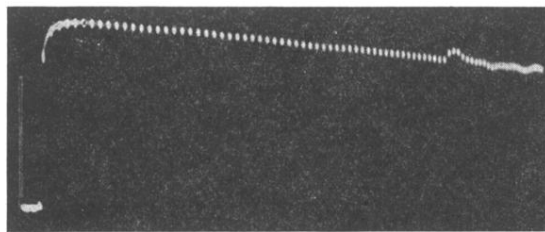


FIG. 2. Second sound pulse in liquid helium *II* (data of June 1, 1948). Sweep proceeds from extreme left where generating voltage pulse appears via pick-up. Received signal occurs at right. Intermediate region represents ambient temperature (slope is due to amplifier recovery from initial pulse). Markers represent 61.1  $\mu$ -second intervals. Additional faint signals indicate conversion between first and second sound.



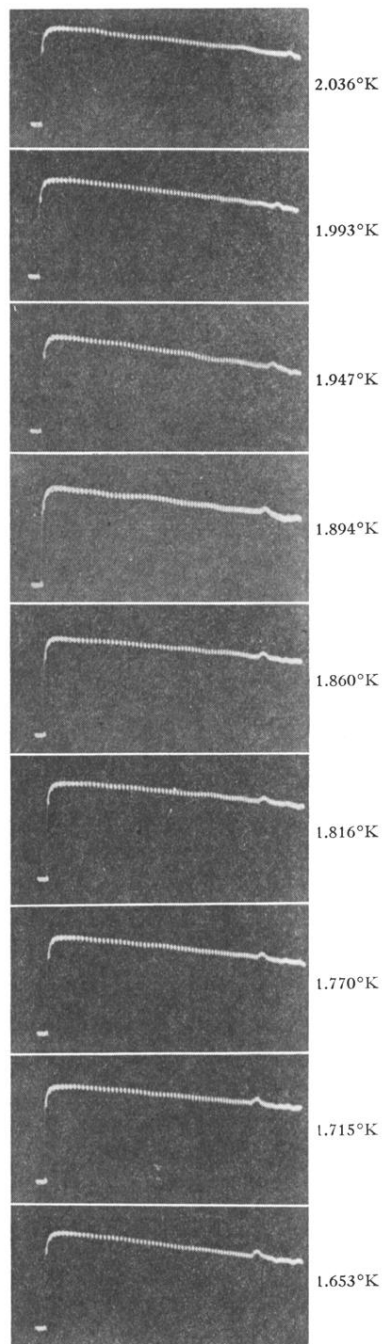


FIG. 7. Second sound pulses at various temperatures for fixed transmitter-receiver distance of 7.57 centimeters (data of June 2, 1948). The trend with temperature is evident.